Mon. Not. R. Astron. Soc. **000**, 1–18 (2005) Printed 5 February 2008 (MN LATEX style file v2.2)

Finding benchmark brown dwarfs to probe the sub-stellar IMF as a function of time.

D. J. Pinfield[1⋆], H. R. A. Jones[1], P. W. Lucas[1], T. R. Kendall[1], S. L. Folkes[1],
A. C. Day-Jones[1], R. J. Chappelle[2] and I. A. Steele[3]
[1] *Centre for Astrophysics Research, Science & Technology Research Institute, Department of Physics Astronomy & Mathematics, University of Hertfordshire, College Lane, Hatfield, Hertfordshire, AL10 9AB, UK*
[2] *Astronomical Institute, Academy of Sciences of the Czech Republic, Bocni II/1401a, 141 31 Prague, Czech Republic*
[3] *Astrophysics Research Institute, Liverpool John Moores University, Twelve Quays House, Egerton Wharf, Birkenhead, CH41 1LD*

Received in original form July 2005

ABSTRACT
Using a simulated disk brown dwarf (BD) population, we find that new large area infrared surveys are expected to identify enough BDs covering wide enough mass–age ranges to potentially measure the present day mass function down to $\sim$0.03M$_{\odot}$, and the BD formation history out to 10 Gyr, at a level that will be capable of establishing if BD formation follows star formation. We suggest these capabilities are best realised by spectroscopic calibration of BD properties ($T_{\rm eff}$, g and [M/H]) which, when combined with a measured luminosity and an evolutionary model can give BD mass and age relatively independent of BD atmosphere models. Such calibration requires an empirical understanding of how BD spectra are affected by variations in these properties, and thus the identification and study of "benchmark BDs" whose age and composition can be established independently.

We identify the best sources of benchmark BDs as young open cluster members, moving group members, and wide (>1000AU) BD companions to both subgiant stars and high mass white dwarfs (WDs). To accurately asses the likely number of wide companion BDs available we have constrained the wide L dwarf companion fraction using the 2MASS All Sky Survey, and find a companion fraction of $2.7^{+0.7}_{-0.5}$% for separations of $\sim$1000–5000AU. This equates to a BD companion fraction of 34^{+9}_{-6}% if one assumes an α $\sim$1 companion mass function. Using this BD companion fraction we simulate populations of wide BD binaries, and estimate that 80^{+21}_{-14} subgiant–BD binaries, and 50^{+13}_{-10} benchmark WD–BD binaries could be identified using current and new facilities. The WD–BD binaries should all be identifiable using the Large Area Survey component of the UKIRT Infrared Deep Sky Survey, combined with the Sloan Digital Sky Survey. Discovery of the subgiant–BD binaries will require a NIR imaging campaign around a large ($\sim$900) sample of Hipparcos subgiants. If identified, spectral studies of these benchmark brown dwarf populations could reveal the spectral sensitivities across the $T_{\rm eff}$, g and [M/H] space probed by new surveys.

Key words: stars: low-mass, brown dwarfs — stars: fundamental parameters — surveys

1 INTRODUCTION

1.1 The IMF and formation history

The initial mass function (IMF) and formation history are the most important observational results produced by the process of Galactic star formation. These two observational cornerstones provide a test-bed for our theoretical understanding of this process. Brown dwarfs (BDs; mass<0.075M$_{\odot}$) populate the lowest mass extreme of the IMF, and current theory suggests that the form of the IMF in this mass range could be particularly sensitive to the initial conditions prevalent for low-mass objects. For instance, Delgado-Donate et al. (2004) predicts a higher fraction of

⋆ E-mail: dpi@star.herts.ac.uk

BDs for a shallower initial slope of the turbulent velocity spectrum in the formation cloud. Bate & Bonnell (2005) suggests that in denser clouds, with lower mean thermal Jeans mass, more BDs will form relative to stars. Chabrier (2003) presents observational evidence suggesting a possible increase in the characteristic mass of star formation that decreases over time, between conditions characteristic of the spheroid (or thick disk) to present-day conditions. Alternatively, Ashman (1990) describes how significant populations of halo (or thick disk) BDs may have formed in cooling flows, and discusses the possibility of a pressure dependent IMF.

One can measure the BD IMF in open clusters as well as younger pre-main sequence clusters emerging from their nascent clouds. However, Lada & Lada (2003) found that the birth rate of embedded clusters exceeds that of visible open clusters by an order of magnitude or more, and that less than 4–7% of embedded clusters survive emergence from molecular clouds to become bound clusters. The most complete way, therefore, of measuring the BD IMF is from the local disk population itself. Furthermore, if BD formation rates are significantly affected by average gas density, pressure and metallicity ([M/H]) in a different way to star formation rates, then we would expect the BD formation history and [M/H] distribution to be sensitive to these factors, and differ in a characteristic way to the stellar distributions.

Measuring these distributions is a major challenge. The nature of BD evolution (cooling and fading with time) means that the mass-luminosity relation depends strongly on age, and one cannot determine either mass or age from a BD's luminosity alone. The usual approach to this problem is to fit synthesised $T_{\rm eff}$ and luminosity functions (constructed with different IMFs and formation histories) to observed BD populations (Allen et al. 2005; Deacon et al. 2005). However, this method is sensitive only to quite drastically different formation histories (eg. one can discriminate between a single halo burst of BD formation 9-10 Gyr ago and a uniform BD birth rate), and then only if one assumes a non evolving IMF (Burgasser 2004). This method also has little chance of constraining the BD [M/H] distribution.

It is a particularly important time for this field, because large scale near infrared (NIR) surveys (currently championed by the 2-Micron All Sky Survey – 2MASS; Skrutskie et al. (1997), and the Denis survey; Epchtein (1997)), are being taken to larger telescopes, with the start of the "UKIRT Infrared Deep Sky Survey" (UKIDSS) on the UK Infrared Telescope, the capabilities of the WIRCam instrument on the Canada France Hawaii Telescope, and the approach of the "Visible and Infrared Survey Telescope for Astronomy" (VISTA). This paper will, in part focus on UKIDSS, as this large scale 7000 square degree survey (Hambly 2003) has well defined parameters and sensitivities. It consists of several sub-surveys (varying in sky coverage and depth), the largest of which is the "Large Area Survey" (LAS) covering 4000 sq degs in four NIR bands, with photometric limits ∼4 magnitudes fainter than 2MASS.

1.2 Aims and paper structure

In light of the significant advances in survey facilities, we would like to more ambitiously assess the issue of how best one could measure the disk BD IMF, formation history and [M/H] distributions. Ideally, one needs a method to directly measure the mass, age, and composition of the individual BDs making up the local disk population. Disk BDs are generally very cool objects with dusty upper atmospheres, comprising very young M dwarfs, a subset of L dwarfs (2300–1300K; Kirkpatrick et al. (1999)) and all T dwarfs (1300–700K; Burgasser et al. (1999)). In general, to determine a BD's mass, age and composition, one must measure $T_{\rm eff}$, g and [M/H] from spectral properties. However, this requires detailed knowledge of the spectral dependencies on these properties, which must come from either theoretical models or the spectroscopic study of a varied population of BDs with well constrained physical properties. Such BDs could be used as fiducial calibrators in $T_{\rm eff}/g/$[M/H] space, and we thus refer to them as *benchmark brown dwarfs*.

In this paper we consider the best types of benchmark BD, and estimate the number of benchmarks that could be found in near future surveys, as well as the range of physical properties that these benchmarks could have. We also compare the expected benchmark properties to those likely amongst the BD populations from the new surveys, and discuss the implications for calibrating the IMF and formation history. In Section 2 we use a simulation of the local disk low-mass population to define the BD mass–age range over which current and future surveys are able to detect enough BDs to constrain the IMF and formation history. In Section 3 we discuss previous work on BDs with constrained properties, the search for sensitive spectral features, and how one could build on this by identifying new types of benchmark BDs with better constrained properties. Sections 4, 5, 6 and 7 discuss these benchmark populations in more detail, and combine new observational results with simulations to estimate the numbers of benchmark BDs that could be discovered in the near future. Section 8 discusses the distribution of the predicted benchmark BDs in mass/age/[M/H] space, comparing these properties with the survey parameter space defined in Section 2. Section 9 contains our conclusions.

2 NIR SURVEY SENSITIVITIES TO THE IMF AND FORMATION HISTORY

2.1 A simulation of disk brown dwarfs

In order to determine the region of the sub-stellar mass–age plane that we expect large scale surveys to probe, we have simulated a local disk population of BDs. We do not intend that this should be a particularly detailed assessment, which would be a sensitive function of the BD population itself (e.g. dependence on structure in the luminosity and $T_{\rm eff}$ functions; Allen et al. (2005)). Instead we consider a particular type of BD population that might be considered "typical" based on current constraints (e.g. Chabrier (2003)). We thus assumed a uniform spatial distribution within the plane itself (ie. uniform surface density), onto which we imposed an α=1 IMF (where $\xi(m) \propto m^{-\alpha}$) and a formation history identical to the local stellar population (Rocha-Pinto 2000). Absolute J-band magnitudes were derived from mass and age, using theoretical models (currently available for solar metallicity; Baraffe et al. (1998); Chabrier et al. (2000a); Baraffe et al. (2003)). We then determine the vertical height above the plane (z) by imposing an exponential z distribution (extending both positive and negative) on the population, which we normalised (for each BD) using the relation

between scale-height (H) and age from Just (2003). We thus account for the fact that disk heating causes older populations to become more vertically dispersed in the disk, with resulting lower number densities in the plane itself (scaling with 1/H(age)). Distances and Galactic latitudes (b) were then derived trigonometrically, and apparent magnitudes determined accordingly. At this point we counted the number of simulated stars out to distances of 20 parsecs with masses from 0.09–0.1$M_\odot$, and normalised the number of objects in our simulation to produce a total of 184 in this mass and distance range, consistent with the observed low-mass stellar mass function (Reid et al. 1999; Chabrier 2001).

2.2 Brown dwarfs in large scale NIR surveys

To select "survey populations" of BDs, we use the sensitivities of 2MASS and the UKIDSS LAS . We selected simulated sub-samples with J$\leqslant$16 and $|b| > 15$ to represent 2MASS BDs, and with J$\leqslant$19.5 and $|b| > 57$ (approximating 4000 square degrees in the Galactic cap) to represent UKIDSS LAS BDs. We also imposed distance limits on our sub-samples. 2MASS allows one to probe for late L dwarfs (M_J ~14.5) out to 20pc, and the UKIDSS LAS will be sensitive to late T dwarfs (M_J ~15.5) out to 50pc. Figure 1 shows the mass–age distribution of our simulated 2MASS (<20pc) and UKIDSS LAS (<50pc) BD samples. Approximate M, L and T spectral type divisions are shown as dotted lines (where class transition $T_{\rm eff}$s were estimated from Knapp et al. (2004)). In the 2MASS figure the 20pc distance limit is essentially the L/T transition. For the UKIDSS LAS, the 50pc distance limit corresponds to a spectral type of ~T7, and is indicated with a dashed line. Note that for the youngest BDs (< a few hundred Myr) the assumption of a uniform spatial distribution where scale height changes cleanly with age will not be ideal, since many very young objects are likely to be in super cluster structures (Montes et al. 2001). The choice of our particular theoretical models is an additional source of uncertainty.

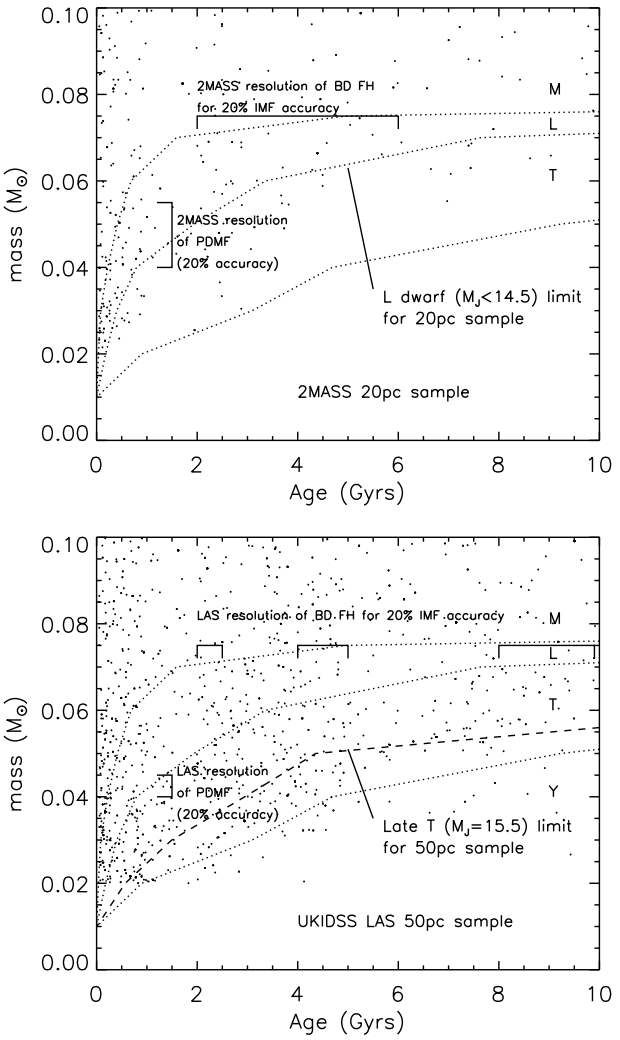

Figure 1. The mass–age plane for low-mass objects in simulated 2MASS and UKIDSS LAS populations. The 2MASS population is an all sky 20pc sample. The UKIDSS LAS population is for 4000 square degrees in the Galactic cap out to 50pc. Estimated spectral class divisions are shown with dotted lines. The 20 and 50pc limits are also shown, corresponding to the L/T transition for 2MASS, and ~T7 for UKIDSS LAS. The resolution of the BD formation history and present day mass function (PDMF) represent age and mass ranges in which the surveys should provide ~ ±20% accuracy (see text).

2.3 The mass-age region probed by surveys

We wish to consider the mass–age region in which we can detect enough BDs to say something specific about their IMF and formation history. As a particularly useful goal, we chose to address the issue of whether one will be able to make a useful comparison between BD formation history and star formation history (which we define using Rocha-Pinto (2000)). This star formation history is characterised by a series of formation bursts (see Burgasser (2004)), lasting 1–3 Gyr, and during which formation rates increase by ~40–50%. To measure such increases we would need an accuracy of ±20% or better in the number of BDs in a particular burst, thus requiring ~25 (assuming Poisson statistics). We indicate in Figure 1 age ranges containing the required number of BDs lying above the completeness limit. We label these age ranges as the resolution of the BD formation history. In a similar, but somewhat more arbitrary way, we indicate a mass range containing ~25 BDs with ages from 0.5–1.5 Gyr (where we exclude the very young BDs for reasons mentioned in Section 2.2) to represent the smallest mass range in which we might constrain the present day mass function (PDMF) with ~20% accuracy. We label this mass range as the resolution of the PDMF.

It can be seen that the 2MASS resolution of the formation history is rather low, and will not be able to resolve star-formation-like bursts of 1-3 Gyr duration. The UKIDSS LAS resolution of the formation history is significantly better, and should be able to constrain bursts of this type even out to the full disk age of ~10 Gyr. The 2MASS resolution of the PDMF is sufficient to constrain its shape at the ΔM~0.015$M_\odot$ level, down to ~0.04$M_\odot$, which could be extended with a closer sample of T dwarfs (eg. Burgasser (2004)). The UKIDSS LAS has a mass resolution 3 times better than this, and should provide a significantly more detailed IMF down to ~0.03$M_\odot$. The mass–age region of in-

terest is thus defined by the UKIDSS LAS 50pc population, lying below the BD limit ($0.075M_{\odot}$) and above the dashed line T7 cut-off in Figure 1b.

3 THE USE OF BENCHMARK BROWN DWARFS

Previously, McGovern et al. (2004) made a spectroscopic study of a selection of youthful late M/early L dwarfs with ages constrained through membership of young associations (1–300Myrs). They compared these spectra to that of an M9.5III+ Mira variable ($\log g \sim 0$) as well as to older disk dwarfs, and found a variety of surface gravity sensitive features, including VO bands (more rounded at lower g), the alkali metal lines KI, RbI, NaI and CsI (weaker at low g), and lithium absorption (stronger for low g) in the optical. They also discovered that in the J-band, very low g causes the appearance of the $\phi(\Delta\nu$=-1) band heads of TiO, the A-X ($\Delta\nu$=-1) band of VO, TiO and VO at 1.14-1.20 microns, and variations in the strength of FeH, KI and H_2O features. Mohanty et al. (2004) has used some of these spectral features (TiO, NaI and KI) to fit $T_{\rm eff}$ and g for 13 very young M5–7.5 dwarfs from the Upper Sco and Taurus star-forming regions. The g values they obtain are consistent with isochrone predictions for the cluster members except for the two coolest objects, and it is clearly that our understanding of how low g can affects the spectra of young late M BDs is improving.

However, only a small fraction of BDs have late M spectral type, and as one moves to cooler $T_{\rm eff}$s, BD atmospheres become more dusty. The physics of dust formation in such objects represents a large uncertainty in the atmospheric models of L and T dwarfs, as well as having a profound effect of the emergent spectra. Observationally, there is a significant spread in L and T broad band colours (Golimowski et al. 2004; Leggett et al. 2002; Cruz et al. 2003) that does not correlate with changes in spectral type. Knapp et al. (2004) noted that the scatter seen in the H-K colour of a sample of T dwarfs showed a correlation with the strength of the KI doublet – a feature expected to be g sensitive. Some L dwarfs also stand out by there surprisingly blue colours, and show enhanced FeH, KI and H_2O. This has been interpreted as resulting from a high g atmosphere depleted of dust due to a higher rate of "rain-out". In this interpretation the amount of dust induced reddening that an L dwarf spectrum undergoes would be highly sensitive to g. Two L dwarfs with halo kinematics also show particularly unusually blue near infrared colours (Burgasser et al. 2003a, 2004) . These objects also show strong FeH features, and are thought to be extremely metal poor halo subdwarfs, where H_2 absorption is depressing the H- and K-band fluxes. Thus, the indications are that the spectral properties of L and T dwarfs are highly sensitive to g and [M/H], as well as to $T_{\rm eff}$.

Despite this potentially promising situation, it is not currently possible to fit L and T dwarf $T_{\rm eff}$, g and [M/H] from spectral synthesis. Atmospheric models that assume a photospheric dust distribution in equilibrium with the gas phase show significant discrepancies for $T_{\rm eff}$ <1800K ($\geqslant$L3; e.g. Leggett et al. (2001)). More sophisticated treatments of dust have since provided broader agreement between theory and the bulk properties of L and T dwarfs, although many uncertainties remain. For instance, fits to theoretical model colours (Marley et al. 2002) of the T dwarf Gl 570D (Knapp et al. 2004) suggested a $T_{\rm eff}$ of $\sim$950K. However, independent constraints placed on this T dwarf from its companion stars indicate a $T_{\rm eff}$ of 784–824K (Geballe et al. 2001). Also, while the latest models of Borrows Sudarsky & Hubeney (2006) show a reasonable correspondence between theoretical spectra and some observations, they also show a variety of discrepancies (e.g shape discrepancies in the H and K bands, and deviations in the Y/Z peak), and are unable to fit the colours of the latest L dwarfs.

To properly understand the sensitivity of both broad band and narrower band spectral features to variations in $T_{\rm eff}$, g and [M/H], it seems clear that one needs to spectroscopically study larger samples of benchmark BDs with more tightly constrained properties. Although brighter benchmark targets would allow for higher signal-to-noise (SN), higher resolution studies, the significant broad band variations in L and T dwarf colour and band strengths can easily be measured at low resolution, and signal-to-noise of $\sim$20–30. Benchmark BDs could thus be as faint as J$\sim$20, and still be studied spectroscopically. J-band spectra (R$\sim$500, SNR$\sim$20) could constrain spectral features at the level of atomic lines and can be measured in $\sim$2hr on an 8m telescope, and even for the blue T dwarfs one should be able to measure K-band spectra (R$\sim$100, SNR$\sim$20) sufficient to accurately constrain the continuum shape in a reasonable time. It is, however, important that the benchmark objects have well known distances, so that their luminosities can be determined. Their age must also be well constrained so that their radii and in particular their mass can be estimated from evolutionary models (although note that L and T dwarf radii are largely, but not totally, independent of mass and age, within a range of $\sim$30%). The $T_{\rm eff}$ and g can thus be determined (from luminosity and radius, and mass and radius respectively), and if [M/H] is also known, then the benchmark BDs will have the full complement of atmospheric properties. Evolutionary models are broadly consistent with each other and observations, and it is thus highly desirable that the atmospheric properties derived rely on evolutionary models as opposed to atmosphere models.

The best places to find such populations of benchmarks are;

- In open clusters, whose age, composition and distance may be well known.
- As nearby members of kinematic moving groups which have known age and composition.
- In well separated multiple or binary systems, where the age, distance, and possibly the metallicity can be inferred through association with the companion stars.

4 BENCHMARK BROWN DWARFS IN OPEN CLUSTERS AND MOVING GROUPS

Young benchmark BDs may be found in open clusters, where the stellar membership is well studied and composition and age are well constrained by e.g. measuring the upper main sequence turnoff (Sarajedini et al. 1999) or the magnitude of the lithium depletion edge (Stauffer Schultz & Kirkpatrick

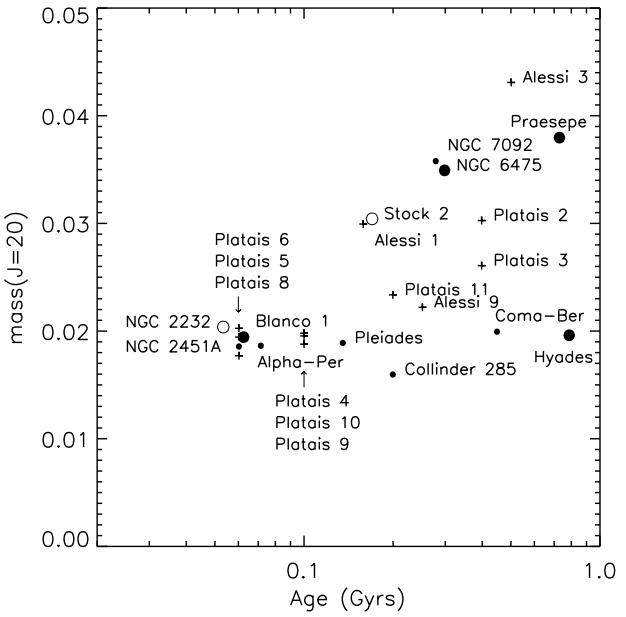

Figure 2. The J=20 mass limit for open clusters from Dias et al. (2002). Small filled circles have [M/H]=-0.1–0.1, and larger circles have [M/H]=±0.1–0.2 (filled circles are metal rich and open metal poor). Clusters with unknown [M/H] are shown as plus signs. Where points are congested, cluster names for several plus signs have been grouped together, with an arrow indicating the location of the group.

(1998); Barrado Stauffer & Jayawardhana (2004)). Provided the cluster is not too young (e.g. <50 Myrs), then the age spread (a few Myrs; e.g. Belikov et al. (2000); Park & Sung (2002)) should not cause significant uncertainty in the age of the members. One simply has to confirm cluster membership of a BD using photometry, proper motion and radial velocity. The upper age limit for which cluster BD populations may no longer be easily probed is set by dynamical evaporation of BDs from these environments. By ∼600–800Myr the identification of cluster BDs becomes difficult. This is the age of the Hyades, in which Dobbie et al. (2002b) did not find any BDs in a 10.5 deg^2 survey sensitive to $I \sim 20$. Even with a substantially larger (17.4 deg^2) deeper ($I \sim z \sim 24$) CFHT12K survey, Bouvier et al. (2005) have identified only ∼2 Hyades BDs (confirmed astrometrically), and a similar situation is seen in Praesepe (Chappelle et al. 2005), a cluster of approximately the same age.

At present, the known BD membership in such regions is an excellent source of benchmark objects. Many of the BDs identified in open clusters (e.g. Pleiades, Praesepe, α Per) have been found by deep, wide-field imaging (Bouvier et al. 1998; Moraux, Bouvier & Stauffer 2001; Dobbie et al. 2002a; Chappelle et al. 2005; Barrado et al. 2002). The number of cluster BD benchmarks will increase significantly as the UKIDSS Galactic Cluster Survey (GCS) obtains deep imaging of six young cluster populations. However, the spectral sensitivity of young BDs to large metallicity changes is not addressed by these populations, since they all have broadly solar [M/H] (-0.1–+0.2 dex).

To address this issue further, Figure 2 shows a plot of the theoretical mass limit probed in open clusters to an apparent magnitude limit of J=20, verses cluster age. Clusters within 1Kpc have been taken from Dias et al. (2002). We used the Lyon group models to calculate the mass limits, as well as expected $T_{\rm eff}$s for cluster members at these limits. We only plot clusters in which one could hope to detect L dwarfs down to $T_{\rm eff}$ ∼1800K, and limit the cluster ages to ⩾50 Myrs. [M/H] values from Dias et al. (2002) have been supplemented (and updated in some cases) by additional values from the literature (Castellani et al. 2002; Strobel 1991; Cameron 1985; Jeffries & James 1999; Piatti Claria & Abadi 1995; Claria & Piatti 1996). The plotting symbols represent these [M/H] values, where small filled circles indicate [M/H]=-0.1–0.1, larger filled and open circles indicate clusters that are metal-rich and poor respectively, with [M/H]=±0.1–0.2. Clusters without published [M/H] values are shown as plus signs.

There are 24 clusters in which one could potentially detect benchmark L and possibly T dwarfs, including 5 of the 6 GCS clusters (IC 4665 is just below our age limit). Six of these have near solar [M/H]=-0.1–+0.1, four are slightly metal rich with [M/H]=0.1–0.2, two are slightly metal poor with [M/H]=-(0.2–0.1), and twelve have no [M/H] determination (all twelve are recently discovered clusters from the analysis of Hipparcos and Tycho-2 data; Platais Kozhurina-Platais & van Leeuwen (1998); Alessi Moitinho & Dias (2003)). There are clearly many clusters in which one might detect benchmark BDs. However, we would draw attention to the fact that there are no young clusters with measured [M/H]>0.2 or <-0.2 in which one could detect benchmarks. This lack of known metal rich young clusters is of particular importance since the local young stellar population has [M/H] as high as 0.3 dex (see Edvardsson et al. (1993)). It would thus be desirable to measure [M/H] of the twelve recently discovered clusters, to provide new cluster targets for benchmark searches.

Moving group populations are distinguishable from the field by their astrometric properties. A moving group remains kinematically distinct within the general field population at ages < 1 Gyr, before being dispersed by disk heating mechanisms (e.g. De Simone & Tremaine (2004)). They are thought to originate in the same environment as open clusters. As progenitor gas is cleared by OB star winds, and the natal cluster expands, stars with sufficiently high velocities become unbound and form a young, coeval moving group, possibly leaving behind a bound open cluster (Kroupa Aarseth & Hurley 2001). Before dispersal after ∼1 Gyr, moving groups therefore consist of young populations with characteristic space motions, and membership of such a group can be used to accurately constrain the age and composition of a BD (Ribas 2003; Pokorny et al. 2004).

Confirmation of moving group membership requires accurate space motions (± few km s^{-1}), from proper motions and radial velocities. The measurement of the proper motions of brighter objects should be achievable using existing data (e.g. 2MASS coupled with SuperCOSMOS). Alternatively, near infrared astrometric techniques are capable of centroiding at the 2mas level (Smart et al. 2005), and could be brought to bear on intrinsically fainter (late L and T dwarf) and more distant moving group benchmark candidates, reaching the required level of proper motion accuracy over a fairly short (1–2yr) base-line. Radial velocities should be measurable using NIR echelle spectrographs on 8m tele-

scopes in the near future, which should provide ∼km/s accuracy down to J∼17 for L and T dwarfs. In addition to kinematics, moving group members with ages <1 Gyr should possess many of the differentiative diagnostics applicable to young cluster BDs. Chief among these are the presence of lithium (*via* the 6708Å line, for ages <100 Myr) as well as numerous gravity-sensitive near-infrared spectroscopic features (McGovern et al. 2004).

As observations confirm complete, homogeneous samples of brown dwarfs in young clusters and moving groups, such BDs can be immediately defined as benchmark objects in the <1 Gyr age range.

5 BROWN DWARF COMPANIONS AT WIDE SEPARATION

BD benchmarks do not however, have to be associated with large populations of stars. They could also be members of multiple or binary systems (Geballe et al. 2001; Smith et al. 2003; Kirkpatrick et al. 2001; Wilson et al. 2001). It has been known for some time that the degree of multiplicity amongst very young stars is greater than that of the more evolved field star populations (Leinert et al. 1993; Duquennoy & Mayor 1991), and thus that the majority of binary systems form together in their nascent clouds. Binary components can therefore generally be assumed to share the same age and composition. The usefulness of such BD companions as benchmark objects will depend on the separation of the components (i.e. if the BD companion can be resolved, and a spectra taken), and the accuracy with which one can constrain the age of the star(s) in the system.

It is known that BD companions to F-M main sequence stars are fairly common at separations >1000AU (Gizis et al. (2001) estimated a companion fraction of 18±14%), in stark contrast to the lack of BD companions at very close separation (the so called BD desert at <3AU; e.g. Marcy & Butler (2000)), as well as at larger separations (< a few hundred AU; McCarthy & Zuckerman (2004)). However, this companion fraction was estimated using just 3 companion BDs discovered in a fraction of the sky and confirmed by common proper motion. The uncertainties associated with this value are thus very large due to small number statistics, and we have therefore chosen to re-asses the level of the wide BD companion fraction, to improve these constraints.

To do this we selected all Hipparcos stars out to 50pc with $\pi/\Delta\pi > 4$ and $|b|$ >30 as target primaries, and searched around these for L dwarfs using a 2MASS Gator cone search in the 2MASS All Sky Release. For each target primary we searched out to a separation corresponding to 5000AU at the distance of the star, or a maximum of 300 arcseconds (the Gator limit) for stars within 16.67pc. We searched for sources with J-K⩾1.1 and J⩽16.1, and with either no optical counterpart, or R-K⩾5.5. Sources were then visually inspected using postage-stamp image data from 2MASS, SuperCOSMOS (R-band and, where available I-band) and Sloan DR4 (where available), to ensure a clean photometric candidate sample.

The top left plot in Figure 3 shows our candidates on an M_J, J-K colour-magnitude diagram (CMD), where in each case we have assumed the candidate to be at the distance of its associated primary star. To identify candidates whose colour and magnitude are inconsistent with companionship, we have defined a region (the dashed box) where we expect L dwarfs to lie, using the L dwarf M_J range from Knapp et al. (2004) coupled with positions of previously confirmed companions in our sample (Kirkpatrick et al. (2001) and Wilson et al. (2001)) as a guide, and allowing for some scatter in colour. The 16 candidates companions in our selection box are shown as filled circles in this plot, and described in Table 1. The primary stars for each candidate are described in Table 2. Non-companions are found below our selection box and have J-K∼1.1–1.3. The bottom left plot shows target distance against candidate companion separation, and it can be seen that all but one of the non companion candidates are at a large separation from a relatively nearby star. The characteristics of the non companions are thus entirely consistent with them being background late M and early L dwarfs in a relatively large space volume.

In order to estimate expected levels of contamination amongst our sample, we repeated our candidate identification procedures using the same target areas offset by 25000AU at the distance of each target, since we expect no companions at such large separations (see Figure 9 of Burgasser et al. (2003b)). The resulting candidates from these control fields are shown in the right two plots of Figure 3, and it can be seen that only 1 of these passes our photometric tests, demonstrating clearly that the vast majority of our candidate companions should be genuine.

To further address the credence of our sample we have investigated available astrometry as well as additional photometry and spectroscopy. Candidate 8 has been spectroscopically measured as L3 (see DwarfArchives.org). Five of the candidates (3, 4, 5, 12 and 14) are already confirmed as common proper motion companions by Kirkpatrick et al. (2001) and Wilson et al. (2001). Amongst the remaining objects five (candidates 2,6,8,9 and 10) are covered in the Sloan 4th data release (DR4) which provides optical measurements for three of these (candidates 2,8 and 10). All three have L dwarf colours compared to Fan et al. (2001) and Hawley et al. (2002). Candidates 13 and 16 have optical counterparts in the SuperCOSMOS PossII and UKST I-band scans respectively, which also yield L dwarf like colours. The time base-line available from 2MASS to DR4 for candidate 2 is only 0.27 yr. However, longer baselines of 2.0yr, 6.1yr, 5.7yr and 14.9yr are available for candidates 8, 10, 13 and 16 respectively, from either 2MASS and DR4 or SuperCOSMOS and 2MASS. Taking into account the proper motions of the primary star candidates, we would expect motions of 1.1, 1.7, 2.0 and 2.0 arcseconds between epochs for these candidates respectively.

We used the geomap and geoxytran routines in Iraf (using 10–15 reference stars and an xy-shift/scale and rotation transformation) to transform either the Sloan pixel coordinates onto a 2MASS frame, or the 2MASS pixel coordinates onto a Schmidt frame. We found typical residuals of ±0.2–0.3 arcseconds in our coordinate transforms, and estimate centroiding accuracies of ±0.1–0.3 arcseconds depending on source brightness. As an additional test to estimate total astrometric uncertainty (including any chromatic effects in the astrometry of these very red sources), we derived the proper motion of candidates 8 and 10 using the full range

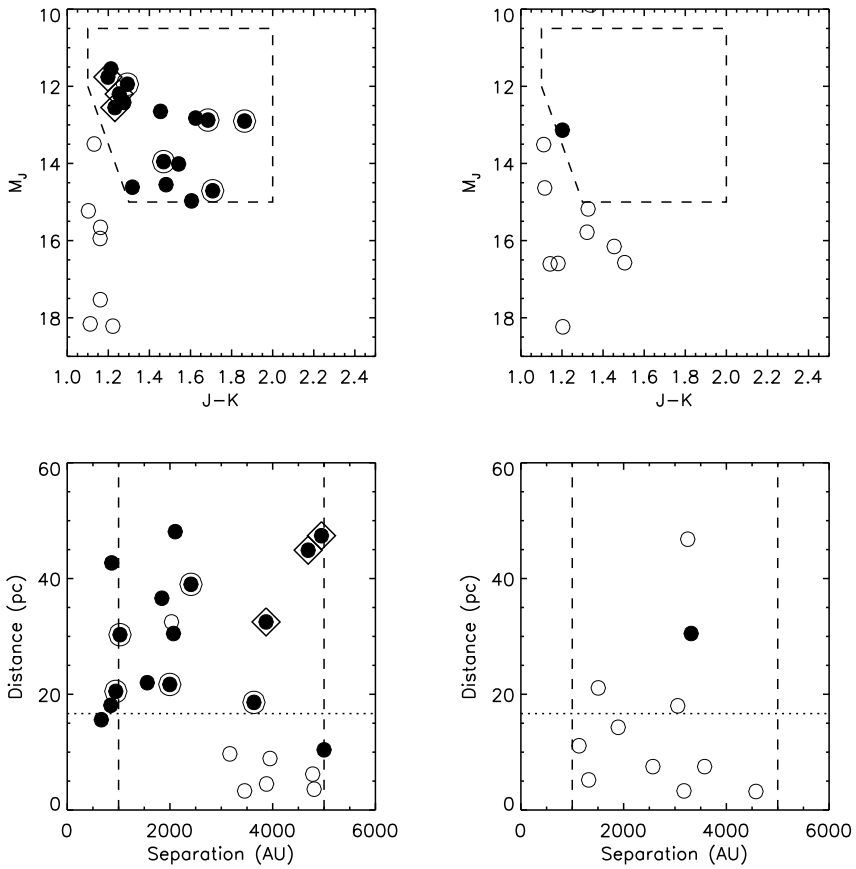

Figure 3. M_J verses J-K colour–magnitude diagrams (top) and distance–separation plots (bottom) for candidate wide L dwarf companions to Hipparcos stars (left) as well as those identified in a set of control fields, offset by 25000AU at the distance of each Hipparcos target. Filled symbols are candidates that pass our L dwarf photometric selection criteria (dashed box in top plots), assuming that the candidate is at the same distance as the primary star. Over-plotted circles and diamonds highlight companions confirmed through common proper motion from the literature and this work respectively (see text). Dotted lines in the bottom plots indicate the distance of 16.67pc and the separation range 1000–5000AU.

of first epoch J, H and K images, and second epoch r', i' and z' images. This analysis suggests an over-all astrometric uncertainty of $\sim \pm 0.7$ arcseconds, in reasonable agreement with our previous estimates.

The final proper motion determinations are shown in Figure 4. The candidate primary proper motions from Hipparcos are shown as circles, and the L dwarf candidate companions as squares. Each primary and candidate secondary are joined by a line for clarity. It can be seen that candidate 8 has large uncertainties, which is because the expected motion over the relatively short 2 yr baseline is comparable to the size of the astrometric uncertainties. Candidates 10, 13 and 16 show significant proper motion, consistent with that of the primary star in each case. These candidates are thus identified as common proper motion companions to HD 120005 (an FV spectroscopic binary), Gl 605 (an M0 dwarf) and HD 216405 (a K1/K2 double star) respectively, and are listed in Table 1 as HD 120005C, Gl 605B and HD 216405C. It is thus clear from the information presented in Figure 3 and Table 1 that our wide binary companion sample is robust.

With this greatly increased number of wide companions, we have been able to place significantly better constraints on the wide BD companion fraction than previously. Using the 14 candidates with distance >16.67pc for which our 2MASS search will be complete out to 5000AU, we have combined the value of M_J for each companion with our J=16.1 search limit to determine the distance out to which we could have detected each companion. We then counted the number of Hipparcos targets out to this distance, establishing the number of stars (n_{stars}) around which a companion could have been detected. We then estimated the L dwarf companion fraction by determining the value of $1/n_{stars}$ for each companion, and summing over all the companions. Finally, we made a small correction by subtracting off $1/n_{stars}$ for the 1 object selected in our control fields. Our final L dwarf companion fraction is $2.7^{+0.7}_{-0.5}$%, where the uncertainties are ± 1-σ assuming binomial statistics. This value is somewhat higher than the Gizis et al. (2001) estimate, although it is consistent to within their large uncertainties. If we assume that the fraction of BDs that can be detected as L dwarfs is 0.08 (for a companion MF with $\alpha \sim 1$; see Gizis et al. (2001)), then we obtain a BD wide companion fraction of 34^{+9}_{-6}%. This is somewhat higher than the wide stellar companion fraction over this separation range (10-15%; Duquennoy & Mayor (1991)), suggesting that wide

Table 1. Wide companion L dwarf candidates.

Cand	2MASS source	Companion name (if confirmed) and notes	J	H	K	M_J^d	J-K	a(AU)
1	2MASS J02124236+0341004		14.70±0.03	13.91±0.04	13.38±0.04	14.62	1.32	5000
2	2MASS J08444996+5532121	[h]	14.70±0.04	13.95±0.04	13.49±0.02	11.55	1.21	865
3	2MASS J09121469+1459396	Gl 337C[b]	15.51±0.08	14.62±0.08	14.04±0.06	13.95	1.47	946
4	2MASS J10221489+4114266	HD 89744B[b]	14.90±0.04	14.02±0.03	13.61±0.04	11.95	1.29	2409
5	2MASS J11122567+3548131	Gl 417B[a]	14.58±0.03	13.50±0.03	12.72±0.03	12.90	1.86	1997
6	2MASS J11451802+0814414		15.47⋆	16.13⋆	14.01±0.06	12.65	1.45	1842
7	2MASS J12201925+2636278		15.83±0.16	13.97⋆	14.55⋆	12.42	1.28	2102
8	2MASS J13204427+0409045	[e,i]	15.25±0.05	14.30±0.03	13.62±0.05	12.82	1.62	2069
9	2MASS J13282546+1346023		15.84±0.16	13.96⋆	14.36⋆	14.55	1.48	848
10	2MASS J13460815+3055038	HD 120005C[c,j]	15.46±0.06	14.81±0.06	14.21±0.06	12.20	1.25	4691
11	2MASS J13471545+1726426		15.94±0.20	14.00⋆	14.33⋆	14.97	1.61	664
12	2MASS J15232263+3014562	Gl 584C[a]	16.06±0.10	14.93±0.08	14.35±0.07	14.71	1.71	3635
13	2MASS J15575569+5914232	Gl 605B[c,f]	14.32±0.03	13.61±0.04	13.12±0.03	11.76	1.20	3871
14	2MASS J16202614-0416315	Gl 618.1B[b]	15.28±0.05	14.35±0.04	13.60±0.04	12.88	1.69	1027
15	2MASS J17420515+7208002		15.73⋆	15.92⋆	14.18±0.07	14.01	1.54	1558
16	2MASS J22530539-3751335	HD 216405C[c,g]	15.93±0.08	15.35±0.09	14.70±0.09	12.55	1.23	4950

Notes:
⋆: 95% confidence upper limit.
[a]Kirkpatrick et al. (2001). [b]Wilson et al. (2001). [c]This work. [d]Assuming the same distance as the primary.
[e]L3 (DwarfArchives.org). [f](R-K)∼7. [g](I-K)∼6. [h](i'-J)=4.3, (i'-z')=2.0.
[i](i'-J)=4.5, (r'-i')=2.4, (i'-z')=1.8. [j](i'-J)=4.2, (r'-i')=2.7, (i'-z')=1.9.

Table 2. Primary star properties for the candidate systems.

Cand	Name	Hip	D(pc)	Spec Typ	V	M_V	B-V
1	Gl 87	10279	10.4	M1.5	10.04	9.95	1.43
2	HD 74150	42919	42.7	K0III-IV	8.91	5.76	0.80
3	Gl 337AB	45170	20.5	G9V/G9V	6.49	4.93	0.73
4	HD 89744	50786	39.0	F7IV-V	5.73	2.77	0.53
5	Gl 417	54745	21.7	G0V	6.41	4.73	0.60
6	HD 102124	57328	36.6	A4V	4.84	2.02	0.17
7	HD 107325[a]	60170	48.1	K2III-IV	5.52	2.11	1.09
8	HD 116012	65121	30.5	K2V	8.58	6.16	0.94
9	Gl 512.1	65721	18.1	G5V	4.97	3.68	0.71
10	HD 120005[b]	67195	44.9	F5	6.51	3.25	0.49
11	Gl 527A[a]	67275	15.6	F6IV	4.50	3.53	0.51
12	Gl 584AB	75312	18.6	G0V/G3V	4.99	3.64	0.58
13	Gl 605	78184	32.5	M0	10.31	7.75	1.27
14	Gl 618.1[a]	80053	30.3	M0V	10.69	8.28	1.38
15	Gl 694.1A	86614	22.0	F5IV-V	4.57	2.86	0.43
16	HD 216405[c]	113010	47.4	K1/K2V	9.36	5.98	0.88

Notes:
[a]Variable star. [b]Spectroscopic binary. [c]Double/multiple star.

BD companions to main sequence stars could be quite common. However, the assumption that $\alpha \sim 1$ represents an important source of uncertainty in this number. Nevertheless, in the remainder of this paper we will assume a BD wide companion fraction of 34^{+9}_{-6}%.

Further constraints on the companion fraction and its mass distribution can be expected in the near future from the UKIDSS LAS. In way of demonstration we have simulated a population of BDs around 34% of main sequence Hipparcos stars (estimating observable BD properties in the same manner as in Section 2.1), and estimate that ∼50 L dwarf and 10–20 T dwarf wide companions may be identified. This population will provide improved statistics when estimating the companion fraction, and the spectral type and M_J distributions of these companions will allow some constraints to be placed on the wide companion mass function. More detailed constraints would come from the population of ∼250 L dwarf and ∼150 T dwarf wide companions that could be available to similar photometric depth over the whole sky. The identification of these would require imaging around ∼10,000 Hipparcos stars, a task that would take over a hundred nights of 4m telescope time using a star-by-star approach. However, if facilities such as WFCAM, WirCam or Vista carry out all sky legacy surveys, this large population of wide L and T dwarf companions could be identified.

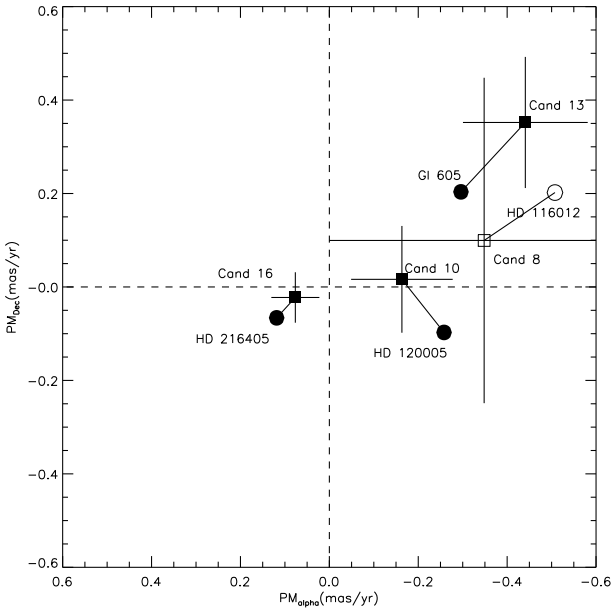

Figure 4. Vector point diagram of the four candidate companions with useful epoch coverage (squares). The proper motions of the candidate primary stars (from Hipparcos) are shown as circles. The open symbols indicate a candidate L dwarf and primary where large measurement uncertainty results in an inconclusive result. The filled symbols indicate measured proper motions consistent with binary pairs. Hipparcos primaries and candidate companions have been joined by solid lines for clarity.

6 BENCHMARK BROWN DWARFS AS WIDE COMPANIONS TO SUBGIANT STARS

Although the ages of main sequence stars are difficult to constrain with great accuracy, this is not the case for subgiants. Once a star has left the main sequence, and thick shell H burning occurs, it evolves almost horizontally across the HR diagram, before reaching the base of the giant branch. During this phase, its age can be accurately determined by comparison with evolutionary models. Theoretical predictions of subgiant evolution are sensitive to [M/H], but since subgiants are pre-dredge-up, [M/H] can be accurately measured, and ages inferred. The largest source of uncertainty in such evolutionary models is the extent of convective core over-shooting (Roxburgh 1989) that occurs for different masses, and this uncertainty is yielding to accurate observational constraints via the study of different aged open clusters (VandenBerg & Stetson (2004) and references therein). Wilson et al. (2001) has identified a wide L dwarf companion to an F7 IV-V primary using 2MASS, and it is clear from their figure 4 that this object gives a much better age calibration (±30% level) than the other 2 binaries reported. However, this star is only just leaving the main sequence, and we expect significantly better age calibration for fully fledged (class IV) subgiants. With [M/H] measured to 0.1 dex (eg. Ibukiyama & Arimoto (2002)), and either distance known to 5% or $\log g$ known to 0.1 dex, subgiant ages can be constrained to $\sim \pm 10\%$ accuracy (Thoren, Edvardsson & Gustafsson 2004).

6.1 Subgiant populations

In order to identify the most comprehensive sample of currently available subgiants for our purposes, we have made use of the Hipparcos database. Figure 5a shows the M_V, B-V diagram of Hipparcos sources with V<13, $\pi/\sigma_\pi \geqslant 4$ and B-V>0.6. Note that even if one has 25% uncertainty on a Hipparcos subgiant parallax, one can subsequently derive an accurate spectroscopic distance, as demonstrated by the spectroscopic distance scale of Fuhrmann (1998), which agrees with Hipparcos parallaxes to an accuracy of 5%. In order to select subgiants from this diagram, we have defined a colour-magnitude selection box using the solar metallicity isochrones of Girardi et al. (2000) as a guide (shown in Figure 5b). We chose the M_V range 2.0–4.5 to include the majority of subgiants while avoiding the brightest ones (where glare would be more of a problem when attempting to image companions) and defined colour cuts to remove the majority of contamination from dwarfs and giant stars. The resulting subgiant selection box is indicated in both these Figures. For different [M/H] the isochrones change, becoming brighter and bluer for lower [M/H]. This means that we expect some contaminating sub-solar metallicity giants in the top right of the selection box. Giants will be undergoing dredge-up and [M/H] calibrations are thus not valid for these stars (Feltzing, Holmberg & Hurley 2001). We have therefore removed any objects that have been spectroscopically flagged as giant-like using data available in the Hipparcos database.

Because we want to identify BDs around these subgiants, we would wish to avoid targets towards reddened regions, and we have thus used the reddening map of Burnstein & Heiles (1982) to identify and remove subgiants where galactic extinction is higher than A_V >0.3 (E_{J-K} <0.05). We would also wish to avoid over-crowded fields, where the extraction of accurate photometry will be problematic because of blended point-source-profiles. We therefore remove subgiants in directions where 2MASS indicates there is >1.1 sources per square arcminute to J=15 (this translates into a typical nearest neighbour distance of <10 arcseconds to J=20; see Section 6.2). The over-crowded regions we avoid include a strip in the Galactic plane, as well as the LMC and SMC. Finally, we remove a small fraction of the subgiants with proper motions <40mas yr^{-1}, since we would wish to follow-up and confirm candidate BD companions by measuring common proper motion. This could be done over a fairly short baseline of 1–2 yrs using adaptive optics imaging facilities such as NAOMI on the William Herschel Telescope, where a proper motion of 40mas/yr would produce a motion on the detector of 1 pixel per year. However, the majority of Hipparcos selected subgiants have proper motions of ∼50-200mas yr^{-1}, and such proper motions could be measured using a more conventional approach. Finally, we impose a distance limit of 160pc on our subgiant sample, designed to facilitate the efficient discovery of approximately equal numbers of L and T dwarf benchmarks (see Section 6.2). Our selection criteria thus identify a target sample of 918 suitable subgiants.

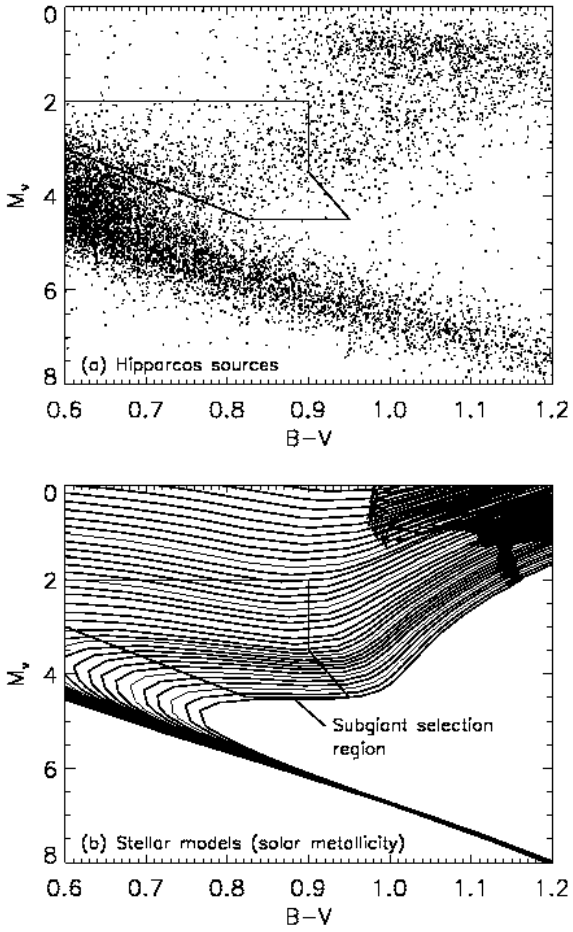

Figure 5. (a) M_V, B-V diagram of Hipparcos stars with V<13 and $\pi/\sigma_\pi \geqslant 4$. (b) Theoretical isochrones from Girardi et al. (2000) for solar [M/H]. Our subgiant colour–magnitude selection box is indicated in both plots.

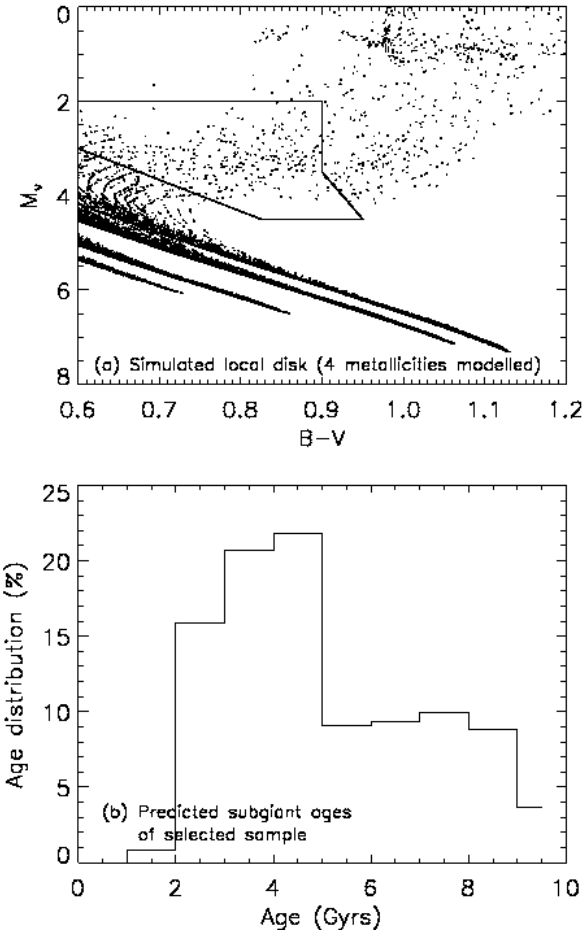

Figure 6. (a) M_V, B-V diagram of our simulated local stellar population (see text). The main sequence appears as four distinct tracks because 4 distinct [M/H] values (0.2, 0.0, -0.35 and -0.65) were simulated (following the distribution of figure 14 from Edvardsson et al. (1993). Our chosen colour magnitude selection box is also shown. (b) The age distribution for the simulated objects extracted from the subgiant selection box.

6.2 Simulating subgiant – brown dwarf binary populations

In order to simulate the properties of BD companions to subgiants, we must estimate an age distribution for the subgiant sample. Because location in the HR diagram depends on several factors ([M/H], mass and age), one cannot simply infer an age distribution from the M_V, B-V diagram. Therefore, we estimated the age distribution using a simulated disk stellar population, for which we assumed a Salpeter MF, a birth rate history from Rocha-Pinto (2000), a disk scale height-age relation from Just (2003) and a metallicity distribution from Edvardsson et al. (1993). Evolutionary tracks (Girardi et al. 2000) were then used to derive the M_V, B-V diagram for a volume limited sample (shown in Figure 6a), from which we selected a simulated subgiant sample using our colour-magnitude selection box to determine the expected age distribution (shown in Fig 6b).

We randomly imposed our predicted age distribution on the subgiant sample, and added BD companions to 34% of these, such that the BD masses follow an α=1 mass function (see Section 5). Lyon group models (see Section 2.1) were then used to derive $T_{\rm eff}$, g and M_J from BD mass and age, and thus J magnitude at the distance of the subgiants.

Figures 7 shows the resulting J magnitude–distance plot for the simulated companion BDs. M L and T dwarf divisions are shown with dotted lines. A photometric limit of J∼20 will allow spectroscopic follow-up of benchmark BDs on 8-m telescopes (see Section 3). We chose a distance limit of 160pc to produce an evenly balanced number of L and T dwarf companions. This region of magnitude–distance space is shown in Figure 7, enclosed by dashed lines.

Our simulation predicts 80^{+21}_{-14} wide companions in this region, approximately equally split between L and T dwarfs. The uncertainty associated with this number comes from the uncertainty of our estimated wide companion fraction (see Section 5).

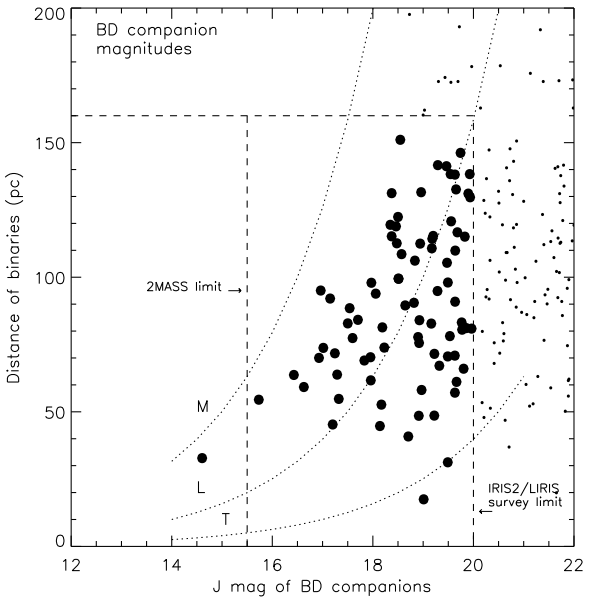

Figure 7. The distance–magnitude distribution of the simulated BD companions to the Hipparcos subgiant population (see text). M, L and T dwarf divisions are shown with dotted lines. Distance–magnitude limits that should provide a good balance of L and T dwarf companions (see text) are indicated with dashed lines. The 2MASS limit is also indicated as a dashed line. The predicted ∼50 companions within these limits are highlighted by filled circles.

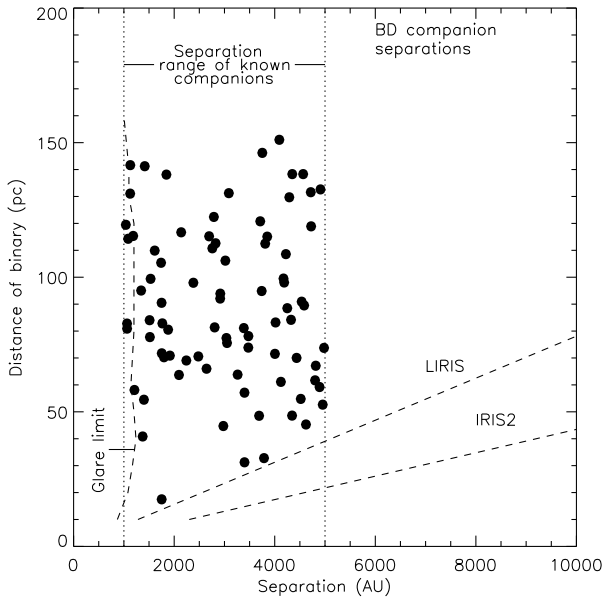

Figure 8. The predicted separation–distance distribution for the subgiant BD companions. The dotted line shows the separation where we expect the PSF wings of typical subgiants to double the sky background in the Y-band. The dashed lines indicate the maximum separations covered by the large format NIR arrays IRIS2 on the AAT and LIRIS on the WHT.

6.3 Finding subgiant brown dwarf binaries

We have shown that $\sim 80^{+21}_{-14}$ L and T dwarfs with J<20 could be expected around a sample of 918 suitable subgiants within 160pc. 2MASS photometry is not deep enough to effectively probe this population (see Figure 5), and although the UKIDSS LAS survey reaches useful photometric depths, it covers only 10% of the sky (and thus ∼10% of the Hipparcos subgiants). Thus the discovery of this benchmark population requires an independent near infrared imaging campaign. Such imaging should be best done in the Y- J- and H-bands (where the Y filter covers the wavelength range ∼0.97–1.07 microns). With separations of ∼1000–5000AU and distances of ∼40-160 parsecs (see Fig 7), the angular separation of these L and T dwarfs from their subgiant primaries should vary from ∼6–125 arcseconds. Charge latency and cross-talk can be a problem when imaging on or near bright sources. But by locating the subgiants a few arcseconds off the edge of an infrared array, it should be possible (with two images – either side of the subgiant) to image ∼95% of the potential companion region, without imaging the subgiant directly.

Glare can also be an issue. The wings of the subgiant PSF will extend for several arcseconds. By assuming a Lorentzian PSF (with ∼1 arcsecond seeing) we have estimated the separation at which PSF brightness is at the same level as typical sky background (in the Y-band, where the sky brightness is lowest). By estimating these separations for our subgiant sample, where we average subgiant brightness as a function of distance, we have defined a minimum separation limit, above which the imaging of faint companions should not be affected by significantly enhanced sky background. This limit is shown in Figure 8 (dashed line), along with the distances and (randomly distributed) separations of the simulated companion population. It can be seen that very few of the companions should be significantly affected by an enhanced sky background. Figure 8 also shows the outer separation limits that would be imposed by NIR arrays the size of LIRIS on the WHT and IRIS2 on the AAT. We thus do not expect companions to be missed by such instruments.

Having imaged candidate wide companions, one needs to be confident that they are genuine, as opposed to random line of sight alignments. We have estimated the likely level of contamination from field objects by working out a contamination volume for each subgiant. We define this volume as that contained in a cone (apex at the observer) that points towards the target, has a cross sectional radius of 5000AU at the target distance, and covers a distance 63%–158% of the target distance. This distance range corresponds to a brightness range of ±1 magnitude, and it should be possible to rule out field BDs in-front of, and more particularly beyond this distance range using colour magnitude information (as was done for the L dwarfs in Section 5). Within our sample contamination volume we have assumed 0.1 BDs per cubic parsec (Reid et al. 1999) and thus expect 12 BDs to be contained in this volume. This number can be directly compared to the 312 BD companions (ie. a 34% companion fraction) around the 918 targets, giving us a contamination fraction of ∼4%. We therefore expect ∼3 field BDs to photometrically contaminate the ∼80 genuine companions. This level of contamination is clearly low, and it is extremely unlikely that any of these contaminating objects would happen to share the proper motion of the primary subgiant. One

should thus be able to confidently confirm such benchmark BDs from their photometry and proper motion.

7 BENCHMARK BROWN DWARFS AS WIDE COMPANIONS TO WHITE DWARFS

The basic physics entering white dwarf (WD) evolution has progressed significantly since the first detailed evolutionary calculations of Lamb & Van Horn (1975). Advances have been made on many fronts, including the convective and conductive opacities, the envelope equation of state, and the thermodynamics of the dense interior plasma including the effects of ion crystallization (see Chabrier et al. (2000a) and references therein). Furthermore, hot WD atmospheres of pure hydrogen can be well modelled (Hubeny & Lanz 1995), and the $T_{\rm eff}$ and g measured accurately by fitting synthetic spectra to Balmer lines in the optical (e.g. Dobbie et al. (2005); Claver et al. (2001)). WD cooling ages can thus be well determined using the measured $T_{\rm eff}$ and g (and an assumed mass–radius relation) and an evolutionary model. It is not, however, possible to establish the [M/H] of a WD progenitor from observations of the WD, since the WD surface composition has little bearing on the progenitor composition.

WD–BD binaries have been the subject of numerous searches in the past. These searches have generally focused on finding resolvable, but relatively close companions. For example, GD 165B was the first of its type discovered, consisting of a WD-L dwarf (probably not quite substellar) binary with a separation of ∼150AU (Zuckerman & Becklin 1992). We do not expect many BD companions to solar type stars at such separations (see Section 5), although less is known about BD companions to higher mass stars (WD progenitors). Note also that when a star becomes a WD, its undergoes mass loss, and during this process any wide companions will spiral out to greater separation (Burleigh, Clarke & Hodgkin 2002). When, for example, a $3M_{\odot}$ star becomes a WD, we expect its mass to decrease by a factor of ∼4 (Williams, Bolte & Koester 2004). Companions separated by 1000–5000AU would spiral out to 4000–20000AU when the star becomes a WD. While some of these binaries may be disrupted due to stellar encounters, we would expect many containing higher mass WDs to remain intact (see figure 9 of Burgasser et al. (2003b)). Previous NIR imaging searches have not effectively probed this very wide separation range – eg. Farihi, Becklin & Zuckerman, (2003) searched for faint companions to WDs within 90 arcsecond separations (<4500AU at the typical 50pc distances of their sample). Wider separation ranges must be searched to identify the very wide binaries in question.

The most important source of uncertainty in the ages of any companions to WDs will generally be the unknown lifetime of the main sequence progenitor star. However, this uncertainty can be minimised by selecting WDs with small progenitor lifetimes. It is known, for example, from the study of open cluster WDs that there is a relationship between the progenitor mass and the WD mass (the so called 'initial-mass-final-mass-relation' or IMFMR), except for a small number of cases where one most likely has a magnetic WD (mass loss may be inhibited by a strong magnetic field). The IMFMR is shown in figure 6 of Williams, Bolte & Koester (2004), and demonstrates that if a WD mass is $>0.7M_{\odot}$, one can place a lower limit on the progenitor mass, and hence an upper limit on the progenitor lifetime, using stellar models.

In order to define good age calibrating WDs, we require the progenitor life-time to be no more than 10% of the WD cooling age. This way, the WD cooling age will be an accurate measure of the total binary age, and hence the age of any BD companion. We show this age calibration criterion on a WD mass–age diagram in Figure 9a. It can be seen that all WD age calibrators have mass$>0.7M_{\odot}$, and that the minimum mass increases for ages <2 Gyr. Figure 9b shows the age calibrating criterion transformed onto a $T_{\rm eff}$–log g diagram, where we overplot WDs from the Sloan first data release (Kleinman et al. 2004). Only ∼15% of these Sloan WDs are good age calibrators, and many of these will have $T_{\rm eff}$ from 7500–10000K (u'-g'∼0.3–0.6, g'-r'∼-0.2–0.3). We thus expect some overlap with the colours of stars (see figure 1 from Smolčić et al. (2004)). Proper motion analysis will thus be an important tool in the identification of age calibrating WDs, allowing selection based on reduced proper motion diagrams (e.g. Knox et al. (1999), Munn et al. (2004)).

7.1 Simulating white dwarf – brown dwarf binary populations

In order to create a synthetic WD disk population, we initially follow the approach of Schroeder Pauli & Napiwotzki (2004; S04). We define a number–distance relation such that $n \propto d^3$ (normalised to 37 WDs within 13pc) out to 50pc. Beyond 50pc we assume that $n \propto d^{2.7}$ to account for reduced number densities as one approaches the average disk scale height of ∼250pc. We define our WD mass distribution using Figure 2 from S04. A complete WD age distribution will be complicated by the time-scales for stellar evolution. However, since we will preselect only WDs that are good age calibrators (ie. with relatively short progenitor life-times), we can make the simplifying assumption that our WD age distribution is the same as the stellar age distribution. We thus assume a WD birth rate identical to the stellar birth rate of Rocha-Pinto (2000), and derive an age distribution by correcting for an age dependent disk scale height, as previously. Synthetic WD properties (luminosity, $T_{\rm eff}$ and g) were derived from mass and age, using equation (1) of S04, and the mass-radius relation of Panei Althaus & Benvenuto (2000).

Simulated WD photometric properties were then determined using a combination of colour–$T_{\rm eff}$ and BC–$T_{\rm eff}$ information from models (Chabrier et al. 2000b) and observation (Kleinman et al. 2004). Photometry was transformed onto the Sloan and photographic systems as required using Bessell (1986) and Smith et al. (2002). Simulated proper motions were also derived by imposing a tangential velocity (V_{tan}) distribution on our population. We assumed an old disk velocity ellipsoid in the UV plane (centred at V,U=-35,0kms^{-1} and with a velocity dispersion of 45kms^{-1}) for ages >1Gyr, and a young disk velocity ellipsoid (U=-20–50kms^{-1}, V=-30–0kms^{-1}) for younger ages. Total proper motions were then determined from V_{tan} and distance. Motion in the UV plane alone will be entirely appropriate when looking in the Galactic cap (i.e. Sloan and UKIDSS LAS), but at lower galactic latitudes we would expect a W compo-

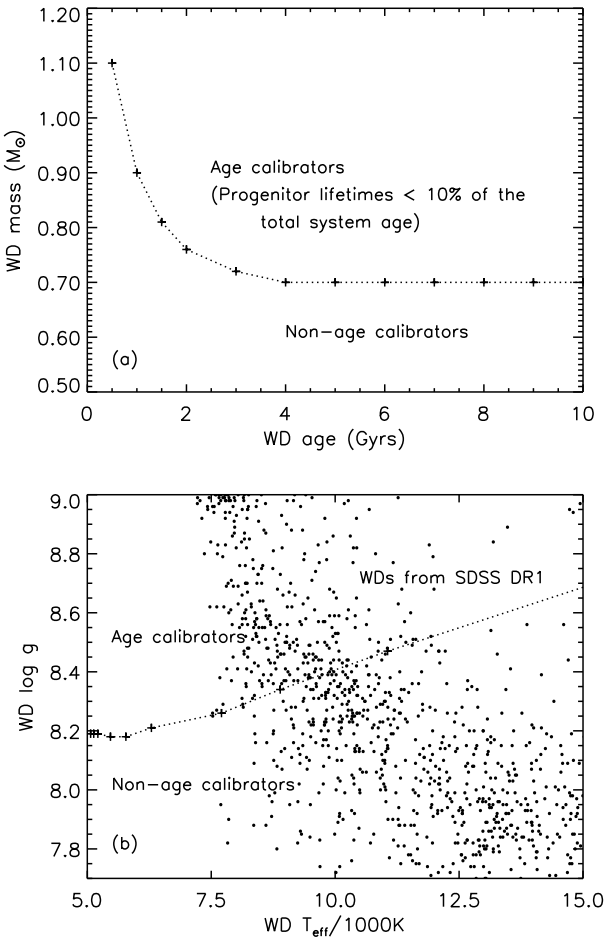

Figure 9. (a) The mass–age plane for WDs. The dotted line indicates where the good age calibrating WDs lie. Above this dotted line, one can place mass constraints on the WD progenitor star that in turn limit its main sequence lifetime to be less than 10% of the WD cooling age. (b) The good age calibration separator (dotted line in (a)) transformed into $\log g$–$T_{\rm eff}$ space. Sloan WDs from Kleinman et al. (2004) are over-plotted.

nent in V_{tan}. However, since it is the size of the proper motions that concerns us (their detectability), estimating the V_{tan} distribution across the whole sky from the UV plane alone should be a good approximation.

We then selected only the good WD age calibrators, using the $T_{\rm eff}$–g criteria from Figure 9, and randomly added wide BD companions to 34% of these, in line with our derived wide companion fraction (see Section 5). An α=1 mass function was imposed on the companion population, and the ages of the BD companions were set to be the same as their WD primaries. BD brightness was then determined from mass and age using the Lyon Group models, and converted to apparent magnitudes using the distance of each binary system.

7.2 Finding white dwarf – brown dwarf binaries in large scale surveys

To determine the number of wide benchmark WD-BD binaries that could be found in large scale surveys, we have extracted photometrically and astrometrically limited samples from our simulated WD-BD population. In the optical, where WDs can be best detected, we consider Schmidt plate surveys covering the whole sky in the B- and R-bands, as well as Sloan which will cover ∼25% of the sky in five bands. SuperCOSMOS for example produces accurate photometry with proper motions uncertainties of ±10mas/yr down to B=19, R=18 (Hambly et al. 2001). With Sloan, one can probe more deeply with accurate proper motions. Munn et al. (2004) combines USNO-B with Sloan to produce a catalogue of absolute proper motions (re-calibrated using Sloan astrometry of galaxies) with improved statistical errors of ∼4mas/yr, due in part to the additional Sloan epoch. This catalogue is 90% complete to g'=19.7. BDs may be selected from Sloan by their large i'-z' colour, where one is limited by i'-band brightness. In the NIR, we consider BDs detected in the 2MASS All Sky Survey, and in the UKIDSS LAS (LAS photometric limits were described in Section 2).

We consider three main survey combinations in which to find benchmark WD-BD binaries. Firstly, one could use 2MASS to find BDs and Schmidt plate photometry and proper motions to identify WDs across the majority of the sky (ignoring regions in the plane and the Magellanic clouds; see Section 6.1). Secondly, one could probe slightly deeper using Sloan+USNO-B to find WDs, and Sloan i'-z' colours to identify BDs (Sloan is sensitive to early L dwarfs out to greater distances than 2MASS). Finally, one could combine the UKIDSS LAS with Sloan+USNO-B, to reach the faintest NIR and optical limits for 10% of the sky. Using the appropriate magnitude limits, requiring that simulated proper motions are $> 5 \times \sigma_{pm}$ (where σ_{pm}=10mas/yr and 4mas/yr for SuperCOSMOS and USNOB+Sloan respectively), and accounting for the fractions of sky covered, we extracted benchmark WD–BD binaries from our simulated population. Our results suggest that one could find ∼9 benchmark systems using 2MASS/Schmidt plate data, ∼6 using Sloan by itself, and $\sim 50^{+13}_{-10}$ benchmark systems from UKIDSS LAS combined with Sloan+USNO-B, where the uncertainties are associated with those of the wide companion fraction (Section 5).

Note that in practise one would also expect to find ∼5 times as many non benchmark WD-BD binaries. For example, there could be ∼300 WD-BD binaries in total amongst the ∼4000 WDs expected in the UKIDSS LAS and USNOB+Sloan combination, with only ∼50 of these systems containing age calibrating WDs and benchmark BDs.

Figure 10 shows BD magnitude against WD magnitude for our simulated wide benchmark binaries in the LAS/Sloan selection. Note that this is for 10% of the sky, and although there are no systems where the BD companion has J<16, the other survey combinations cover a larger area of sky, and are able to identify some brighter BD companions. The main limiting factor for these other combinations is the detection of BDs using 2MASS J or Sloan i'. The significantly greater photometric depth of the LAS provides sensitivity to a much larger number of benchmark systems, and it can be seen that the optical and NIR depths of Sloan and the LAS are quite well matched for this purpose.

We have estimated likely levels of contamination in the simulated LAS/Sloan+USNO-B population as we did for the subgiant companions in Section 6.3. However, note that WD companions are expected to be in wider orbits, so we

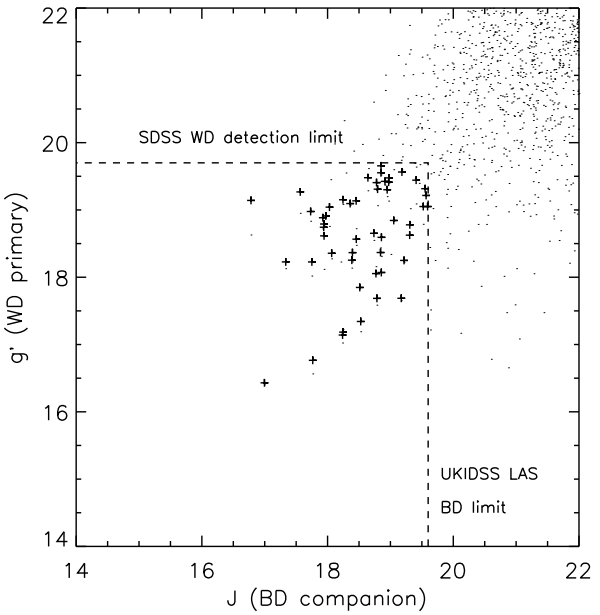

Figure 10. The simulated WD–BD wide binary population from 10% of the sky. Sloan g'-magnitudes for WDs are plotted against BD J-magnitudes. Sloan and UKIDSS LAS photometric limits are indicated with dashed lines. Identifiable benchmark binaries in our simulated population are indicated with crosses.

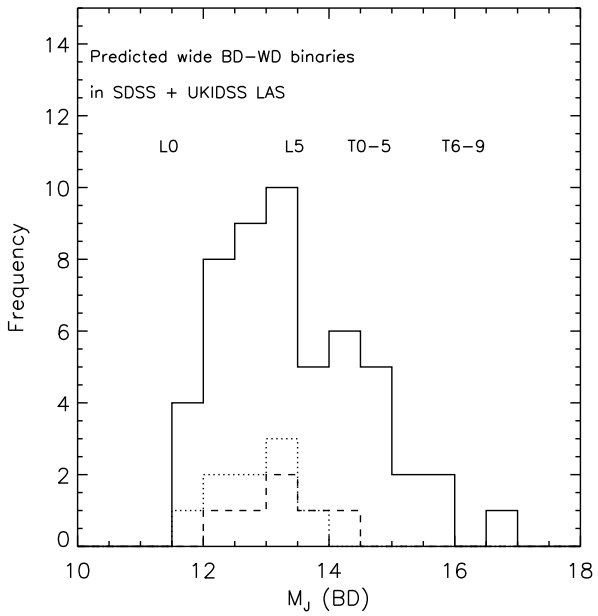

Figure 11. M_J distribution of the simulated wide BD companions to WDs. Those detectable in Sloan combined with the UKIDSS LAS are shown by the solid histogram. Those detectable in 2MASS combined with Schmidt plate coverage, and by Sloan alone, are shown by the dotted line and dashed line histograms respectively. Approximate spectral class locations are indicated at the top of the plot.

assume a cone with a 20000AU radius at the distance of the target. Using the same approach as in Section 6.3 we estimate that ∼400 contaminating field objects will have photometry consistent with companionship. This number is comparable with the expected number of WD-BD binaries (cf. ∼300). Clearly such contamination is more of an issue for these systems than it was for subgiant companions. However, common proper motion should still be a very effective way of confirming genuine binary companions.

7.3 Confirming white dwarf – brown dwarf benchmark systems

Having established companionship through common proper motion, optical spectroscopy of the WDs on 4–8m class telescopes, will allow their $T_{\rm eff}$ and $\log g$ to be measured. This will establish if they are good age calibrators (according to Figure 9b), and allow their cooling ages to be determined. Our simulation suggests that the WD–BD systems will have distances ranging from ∼25–300pc, so although parallax distances could be derived for the closer binaries, alternative WD distance constraints will be required for many, if the BD is to be a benchmark object. Such distance constraints can also come from the $T_{\rm eff}$ and $\log g$ measurements when combined with WD evolutionary models, since together these allow the WD mass and radius (and thus luminosity) to be measured. Such spectroscopically determine properties should be quite robust, as demonstrated by Claver et al. (2001), who studied populations of open cluster WDs and showed that the spectroscopic masses agree very closely with those derived via an assumed cluster distance, and with those derived via gravitational redshifts. With a WD cooling age and spectroscopic or parallax distance for a binary, the BD $T_{\rm eff}$ and $\log g$ can be derived (see Section 3), creating a benchmark BD.

7.4 Spectral types of wide brown dwarf companions to white dwarfs

Figure 11 shows the M_J frequency distribution of the simulated BD companions to WDs from the LAS combined with Sloan+USNO-B simulation (solid histogram). Approximate spectral class locations are indicated near the top of the plot. Also plotted are the frequency distributions for the simulated systems from 2MASS combined with SuperCOSMOS (dotted histogram) and Sloan by itself (dashed histogram). The low numbers of BD companions detectable in the absence of the UKIDSS LAS are mostly L dwarfs. 2MASS/SuperCOSMOS should identify slight more systems, but Sloan may probe to slightly later BDs. However, the simulated population from LAS combined with Sloan covers the M_J=11.5–16 range, corresponding to L–late T. The LAS is clearly vital to both increase the number of WD-BD benchmark systems as well as extending the spectral type range to the later T dwarfs.

8 THE BENCHMARK BROWN DWARFS IN MASS-AGE SPACE

Figure 12 shows the predicted mass-age distribution of the different benchmark populations discussed in this work (annotation is the same as in Figure 1a). The mass-age region in which UKIDSS LAS could accurately measure the BD IMF

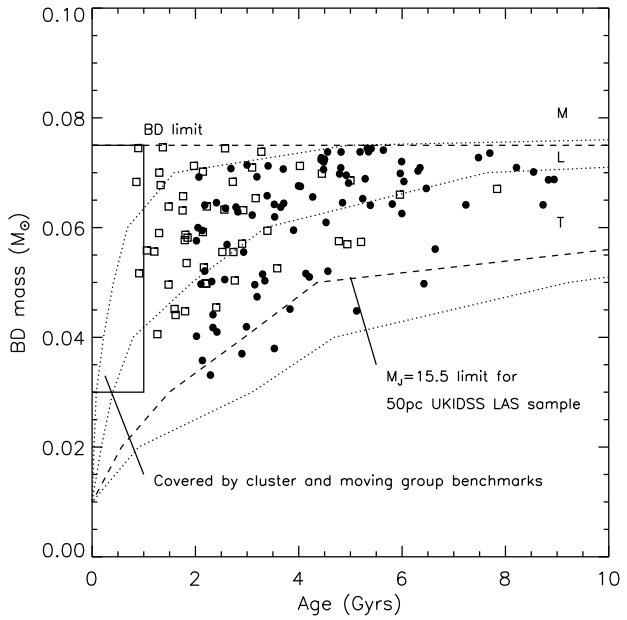

Figure 12. The mass–age distribution of the benchmark BDs discussed in this work. Estimated spectral class divisions are shown with dotted lines. The 50pc limit for ∼T7 dwarfs in the UKIDSS LAS is shown as a dashed line. Together with the BD limit (also a dashed line) these enclose the region in which we expect the UKIDSS LAS to measure the BD PDMF and formation history. The mass–age region covered by young clusters and moving groups is enclosed by the solid line rectangle. Predicted benchmark BDs as wide companions to subgiant stars, and as wide companions to high mass WDs are shown as filled circles and open squares respectively.

and formation history is enclosed by the dashed lines (see Section 2). The mass-age region that we expect to be covered by cluster and moving group benchmarks is indicated by the solid line rectangular box, representing 0.03–0.075$M_\odot$ and <1 Gyr.

The simulated wide binary BD companions to subgiants and high mass WDs are shown as filled circles and open squares respectively. The two types of binary BD have significant overlap in mass-age space. However, note that there are particular mass-age regions that are primarily covered only by one type of binary companion. Due to the deeper coverage of our simulated subgiant survey, the subgiant companions populate the late T dwarf region more effectively than the WD companions found in the LAS (see also Figure 7 and Figure 11). This means that this benchmark population is particularly important in the context of deriving the BD formation history, as well as the lower mass end of the intermediate age disk IMF (eg. 0.04–0.06$M_\odot$, 2–4 Gyr). However, the subgiant benchmarks do not cover the age range <2Gyr (see also Figure 6b). The benchmark WD companions are not very common for ages >5Gyrs. However, they do cover the 1–2 Gyr age range.

It is also important to consider the benchmark BD number density within $T_{\rm eff}$–g–[M/H] space. For the older systems (4–10 Gyr), the relatively small mass range covered (∼0.055–0.075 $M_\odot$) results in a small g range ($\log g \simeq$5.3–5.4), but a large $T_{\rm eff}$ range (∼2000–1000K). In this part of the mass–age diagram, it is important to thoroughly populate the $T_{\rm eff}$–[M/H] plane as much as possible, using the subgiant companion benchmarks. We expect the [M/H] distribution of these benchmarks to follow the [M/H]–age distribution from Edvardsson et al. (1993) (i.e. the [M/H] distribution that we assumed for the subgiant primaries in our simulation). As shown in Figure 14 of Edvardsson et al. (1993), on average there is a slight preference for lower [M/H] systems at older ages. However the spread in [M/H] at all ages is significantly larger than this trend, and for 4–10 Gyr ages [M/H] is quite uniformally spread from ∼-0.7–+0.2 (i.e. a spread of ∼1 dex). Our simulations predict ∼40 subgiant companion benchmarks in this age range, and with the expected $T_{\rm eff}$ and [M/H] distributions we thus expect ∼1 benchmark BD per $\Delta T_{\rm eff}$=200K Δ[M/H]=0.1 dex.

For the younger BDs (1–4 Gyr), the larger mass range covered will result in a larger g range ($\log g \simeq$5–5.3) as well as a large $T_{\rm eff}$ range (∼2000–1000K). It is thus important to more fully populate this part of the mass-age plane, and the ∼80 simulated subgiant and WD companion benchmarks should give ∼1 benchmark BD per $\Delta T_{\rm eff}$=100K, Δg=0.04 dex.

9 CONCLUSIONS

In this paper we have discussed the current prospects for identifying field BD populations, and examined their likely mass, age and [M/H] distribution. We also consider the idea that it may be possible to constrain their properties using a combination of spectroscopically determined $T_{\rm eff}$, g and [M/H] combined with distance constrains and an evolutionary model. We suggest that the spectroscopic calibration of these properties might be realised via the study of populations of BDs whose properties are well constrained by independent means – so called benchmark BDs. We consider the different types of benchmark BDs that could be discovered, the number of benchmarks that we may expect to find in the near future, and the range of properties that we can expect them to have. Our conclusions may be summarised as follows:

- The UKIDSS LAS should discover large numbers of field BDs covering a substellar mass range down to 0.03$M_\odot$ (for ages <1.5Gyr), and an age range out to 10 Gyr (for masses from 0.055 –0.075$M_\odot$).
- The best sources of young (<1 Gyr) benchmark BDs should be in open clusters and moving groups. Some benchmarks of this type are known already, but many more are expected in the next few years from the UKIDSS GCS survey. These clusters all have [M/H]=-0.1–0.2 however, and the [M/H] of additional young clusters must be measured in order to provide hunting grounds for the most metal rich and metal poor young benchmark BDs.
- The best sources of older (>1 Gyr) benchmark BDs should be as wide companions to subgiant stars and high-mass (>0.7$M_\odot$) WDs. BD $T_{\rm eff}$, g and [M/H] can be accurately constrained by association with subgiant companions, and high mass WD companions may be used to constrain BD $T_{\rm eff}$ and g.
- A NIR survey around ∼900 available Hipparcos subgiants could find $\sim 80^{+21}_{-14}$ benchmark BDs. Such benchmark objects will be particularly useful for revealing spectral sensitivities to [M/H], and to the $T_{\rm eff}$ and g of older BDs.

• The combination of the UKIDSS LAS and Sloan surveys could find $\sim 50^{+13}_{-10}$ BD companions to high-mass WDs. These benchmark BDs should be particularly useful for studying the spectral sensitivities to $T_{\rm eff}$ and g of BDs in the 1–2 Gyr age range.

• Together, the available benchmark populations cover the mass–age range in which the PDMF and formation history can be measured. Also, the [M/H] distribution of the benchmark BDs seems likely to encompass the [M/H] range expected amongst field BDs, accepting the caveat about the young cluster benchmarks. BD $T_{\rm eff}$–g–[M/H] space should be well populated by these benchmark objects, which could thus provide a grid of fiducial benchmark BDs for spectroscopic study.

The identification of these benchmark populations could thus provide a foundation to allow the UKIDSS LAS to accurately probe the BD PDMF down to $0.030 M_{\odot}$, and the substellar (0.055–$0.075 M_{\odot}$) formation history from 0–10 Gyr.

ACKNOWLEDGEMENTS

We acknowledge support from PPARC for this work, in particular for their support of DP, PL, TK & SF. This research has made use of data obtained from the Leicester Database and Archive Service at the Department of Physics and Astronomy, Leicester University, UK.

REFERENCES

Alessi, B. S., Moitinho, A., Dias, W. S., 2003, A& A, 410, 565
Allen, P. R., Koerner, D. W., Reid, I. N., Trilling, D. E., 2005, ApJ, 625, 385
Ashman, K. M., 1990, MNRAS, 247, 662
Baraffe, I., Chabrier, G., Allard, F., Hauschildt, P. H., 1998, A&A, 337, 403
Baraffe, I., et al., 2002, A&A, 382, 563
Baraffe, I., Chabrier, G., Barman, T. S., Allard, F., Hauschildt, P. H., 2003, A&A, 402, 701
Barrado y Navascués D., Bouvier J., Stauffer J.R., Lodieu N. & McCaughrean M.J., 2002, A&A, 395, 813
Barrado y Navascués D., Stauffer J.R. & Jayawardhana R., 2004, ApJ, 614, 386
Bate, M. R. & Bonnell, I. A., 2005, MNRAS, 356, 1201
Belikov, A. N., Kharchenko, N. V., Piskunov, A. E., Schilbach, E., 2000, A&A, 358, 886
Bessell, M. S., 1986, PASP, 98, 1303
Bouvier J., et al., 1998, A&A, 336, 490
Bouvier J., Kendall T.R., Meeus G., Stauffer J.R., Cuillandre J.-C. & Bertin E., 2005, in prep.
Burgasser, A. J., et al., 1999, ApJ, 522, 65
Burgasser, A. J., et al. 2003a, ApJ, 592, 1186
Burgasser, A. J., Kirkpatrick, J. D., Reid, I. N., Brown, M. E., Miskey, C. L., Gizis, J. E., 2003b, ApJ, 586, 512
Burgasser, A. J., et al., 2004, ApJ, 614, L73
Burgasser, A. J., 2004, ApJS, 155, 191
Burleigh, M. R., Clarke, F. J., Hodgkin, S. T., 2002, MNRAS, 331, L41
Burnstein, D., Heiles, C., 1982, AJ, 87, 1165
Burrows, A. J., Sudarsky, D., Hubeney, I., 2006, AJ, in press
Cameron, L. M., 1985, A& A, 147, 47
Castellani, V., Degl'Innocenti, S., Prada Moroni, P. G., Tordiglione, V., 2002, MNRAS, 334, 193
Chabrier, G., 2001, ApJ, 554, 1274
Chabrier, G., 2003, PASP, 115, 763
Chabrier, G., Baraffe, I., Allard, F., Hauschildt, P. H., 2000, ApJ, 542, 464
Chabrier, G., Brassard, P., Fontaine, G., Saumon, D., 2000, ApJ, 543, 216
Chappelle R. J., Pinfield, D. J., Steele, I. A., Dobbie, P. D., & Magazzù, A., 2005, MNRAS, in press
Claria, J. J. & Piatti, E. P., 1996, PASP, 108, 672
Claver, C. F., Liebert, J., Bergeron, P., Koester, D., 2001, ApJ, 563, 987
Cruz, K. L., et al. 2003, AJ, 126, 2421
Deacon, N. R., et al., 2005, MNRAS, in prep
Delgado-Donate, E. J., Clarke, C. J., Bate, M. R., & Hodgkin, S. T., 2004, MNRAS, 351, 617
De Simone R., Wu X. & Tremaine S., 2004, MNRAS, 350, 627
Dias, W. S., Alessi, B. S., Motinho, A., & Lépine, J. R. D., 2002, A&A, 389, 871
Dobbie, P. et al. 2002a, MNRAS, 335, 687
Dobbie P., Kenyon F., Jameson R.F., Hodgkin S.T., Hambly N.C. & Hawkins M.R.S., 2002b, MNRAS, 329, 543
Dobbie, P. D., et al., 2005, MNRAS, 335, L39
Duquennoy, A., Mayor, M., 1991, A&A, 248, 485
Edvardsson, B., Andersen, B., Lambert, D. L., Nissen, P. E., Tomkin, J., 1993, A&A, 275, 101
Epchtein, N., 1997, in The Impact of Large-Scale Near-Infrared Surveys, ed. F. Garzón, N. Epchtein, A. Omont, B. Burton, & P. Persi (Dordrecht: Kluwer Academic Publishers), 25
Fan, X., et al. 2000, AJ, 119, 928
Farihi, J, Becklin, E. E., Zuckerman, B., 2003, IAUS, 211, 289
Feltzing, S., Holmberg, J., Hurley, J. R., 2001, A&A, 377, 911
Fuhrmann, K., 1998, A&A, 338, 161
Geballe, T. R., Saumon, D., Leggett, S. K., Knapp, G. R., Marley, M. S., Lodders, K., 2001, ApJ, 556, 373
Girardi, L., Bressan, A., Bertelli, G., Chiosi, C., 2000, A&AS, 141, 371
Gizis, J. E., Kirkpatrick, J. D., Burgasser, A. J., Reid, I. N., Monet, D. G., Liebert, J., Wilson, J. C., 2001, ApJ, 551, L163
Golimowski, D. A., Leggett, S. K., Marley, M. S., Fan, X., Geballe, T. R., Knapp, G. R., 2005, in the Proceedings of the 13th Cool Stars Workshop, ESA Special Publications Series, 575
Hambly, N. C., Davenhall, A. C., Irwin, M. J., MacGillivray, H. T., 2001, MNRAS, 326, 1279
Hambly, N. C., 2003, IAUS, 211, 477
Hawley, S. L., et al. 2002, AJ, 123, 3409
Hubeney, I., Lanz, T., 1995, ApJ, 439, 975
Ibukiyama, A, Arimoto, N., 2002, A&A, 394, 927
Jeffries, R. D., James, D. J., 1999, ApJ, 511, 218
Just, A., 2003, Ap& SS, 284, 727
Kirkpatrick, J. D. et al., 1999, ApJ, 519, 802
Kirkpatrick, J. D. et al., 2001, AJ, 121, 3235

Kleinman, J. J., et al., 2004, ApJ, 607, 426
Knox, R. A., Hawkins, M. R. S., Hambly, N. C., 1999, MNRAS, 306, 736
Knapp, G. R. et al., 2004, AJ, 127, 3553
Kroupa P., Aarseth S. & Hurley J., 2001 MNRAS, 321, 699
Lada, C. J., & Lada, E. A., 2003, ARA& A, 41, 57
Lamb, D. Q., Van Horn, H. M., 1975, ApJ, 200, 306
Leggett, S. K., Allard, F., Geballe, T. R., Hauschildt, P. H., Schweitzer, A., 2001, ApJ, 548, 908
Leggett, S. K., et al., 2002, ApJ, 564, 452
Leinert, Ch., et al., 2005, A&A, 278, 129
Marcy, G. W., Butler, R. P., 2000, PASP, 112, 137
Marley, M. S., et al. 2002, ApJ, 568, 335
McCarthy, C., Zuckerman, B., 2004, AJ, 127, 2871
McGovern, M. R., Kirkpatrick, J. D., McLean, I. S., Burgasser, A. J., Prato, L., Lowrance, P. J., 2004, ApJ, 600, 1020
Mohanty, S., Basri, G., Jayawardhana, R., Allard, F., Hauschildt, P., Ardila, D., 2004, ApJ, 609, 854
Montes, D., López-Santiago, J., Gálvez, M. C., Fernández-Figueroa, M. J., De Castro, E., Cornide, M., 2001, MNRAS, 328, 45
Moraux, E., Bouvier, J., Stauffer, J. R., 2001, A&A, 367, 211
Munn, J. A., et al., 2004, AJ, 127, 3034
Panei, J. A., Althaus, L. G., Benvenuto, O. G., 2000, A&A, 353, 970
Park, B., Sung, H., 2002, AJ, 123, 892
Perryman M. A. C., et al., 1998, A&A, 331, 81
Piatti, E. P., Claria, J. J., & Abadi, M. G., 1995, AJ, 110, 2813
Platais, I., Kozhurina-Platais, V., & van Leeuwen, F., 1998, AJ, 116, 2423
Pokorny, R. S., Jones, H. R. A., Hambly, N. C., Pinfield, D. J., 2004, MNRAS, 355, L39
Reid, I. N., et al., 1999, ApJ, 521, 613
Ribas, I., 2003, A&A, 400, 297
Rocha-Pinto, H. J., Scalo, J., Maciel, W. J., Flynn, C., 2000, ApJ, 531, L115
Roxburgh, I. W., 1989, A&A, 211, 361
Sarajedini A., von Hippel T., Kozhurina-Platais V. & Demarque P. 1999, AJ, 118, 2894
Schroeder, K. -P., Pauli, E. -M., Napiwotzki, R., 2004, MNRAS, 354, 727
Skrutskie, M. F., et al., 1997, in The Impact of Large-Scale Near-Infrared Surveys, ed. F. Garzón, N. Epchtein, A. Omont, B. Burton, & P. Persi (Dordrecht: Kluwer Academic Publishers), 25
Smart, R. L., Bailer-Jones, C. A. L., Jones, H. R. A., 2005, in Proceedings of IAU Colloquium 196, 420
Smith, J. A., et al., 2002, AJ, 123, 2121
Smith, V. V., et al., 2003, ApJ, 599, L107
Smolčić V., et al., 2004, ApJ, 615, 141
Stauffer J.R., Schultz G. & Kirkpatrick J.D. 1998, ApJ, 499, L189
Strobel, A., 1991, Astron. Nachr., 312, 177
Thoren, P., Edvardsson, B., Gustafsson, B., 2004, A&A, 425, 187
VandenBerg, D. A., Stetson, P. B., 2004, PASP, 116, 997
Williams, K. A., Bolte, M., Koester, D., 2004, ApJ, 615, 49
Wilson, J. C., Kirkpatrick, Gizis, J. E., Skrutski, M. F., Monet, D. G., Houck, J. R., 2001, AJ, 122, 1989
Zuckerman, B., Becklin, E. E., 1992, ApJ, 386, 260

This paper has been typeset from a TEX/ LATEX file prepared by the author.